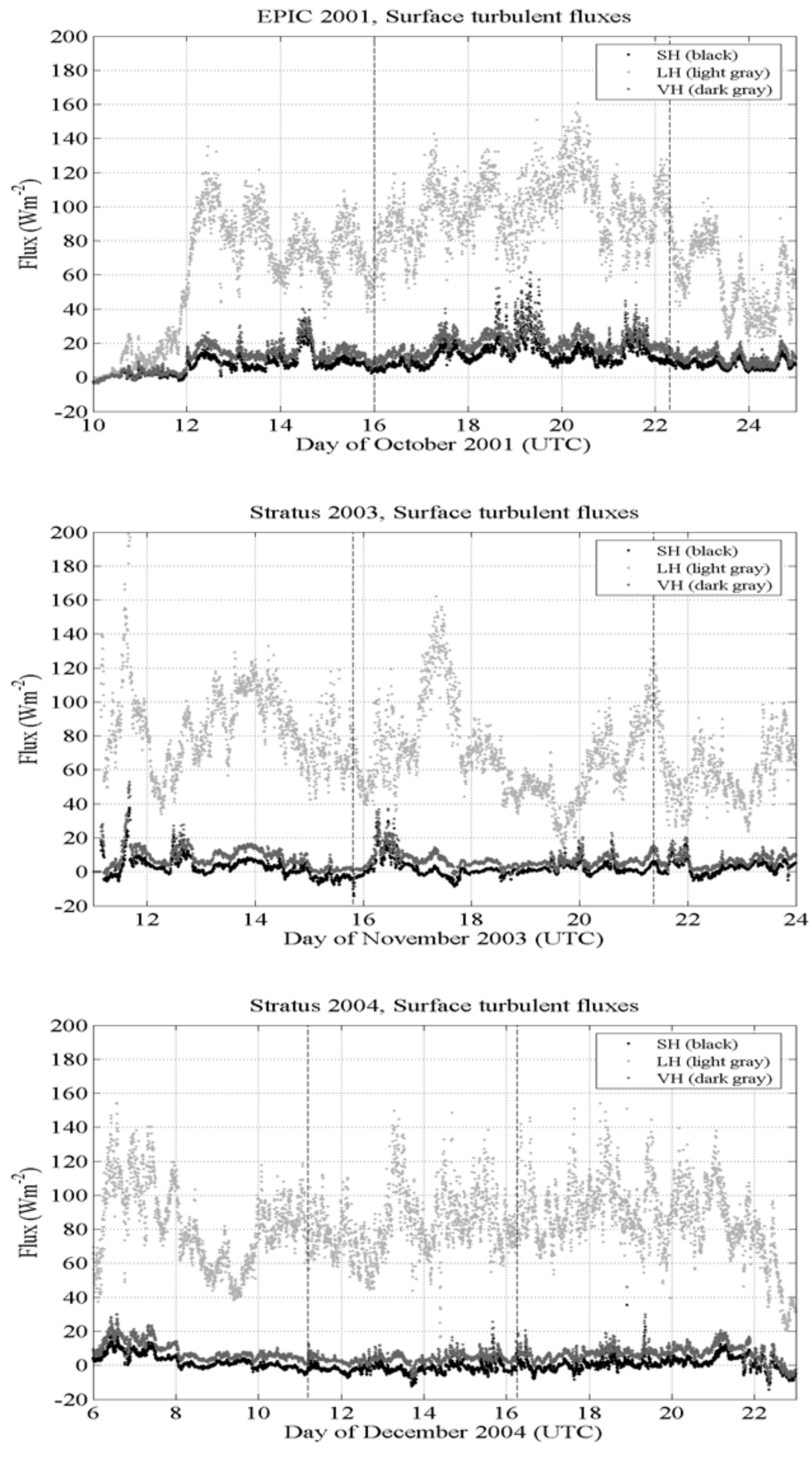

Figure 1. Surface sensible heat (black), latent heat (light gray) and virtual heat (dark gray) fluxes during EPIC (upper panel), Stratus 2003 (middle panel) and Stratus 2004 (lower panel). The temporal resolution is 5 min. Dashed lines indicate the period when the ship was stationed at the WHOI buoy.

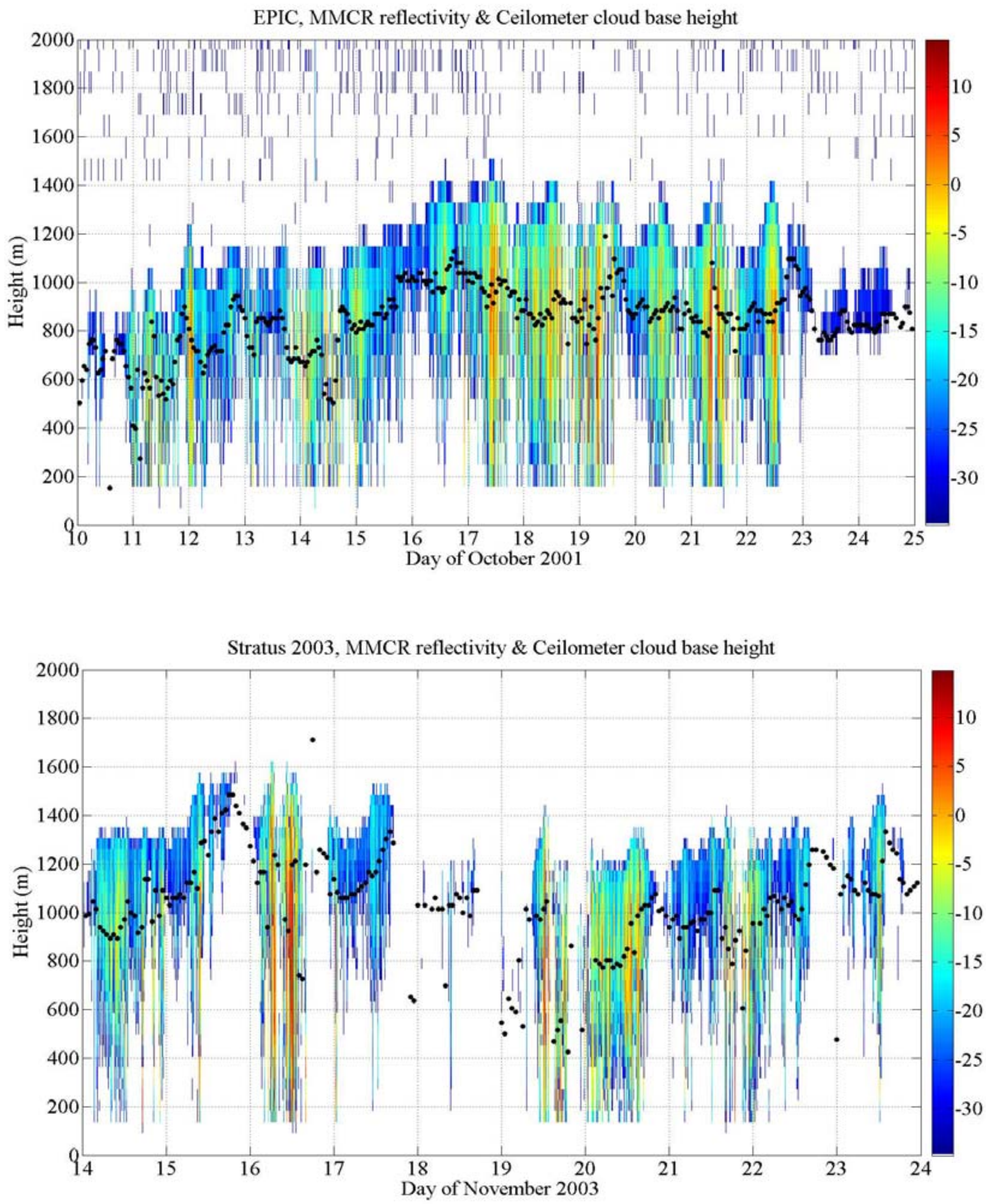

Figure 2. Reflectivity from the MMCR during EPIC 2001 (top) and Stratus 2003 (bottom). The ceilometer cloud base height is shown with the black dots.

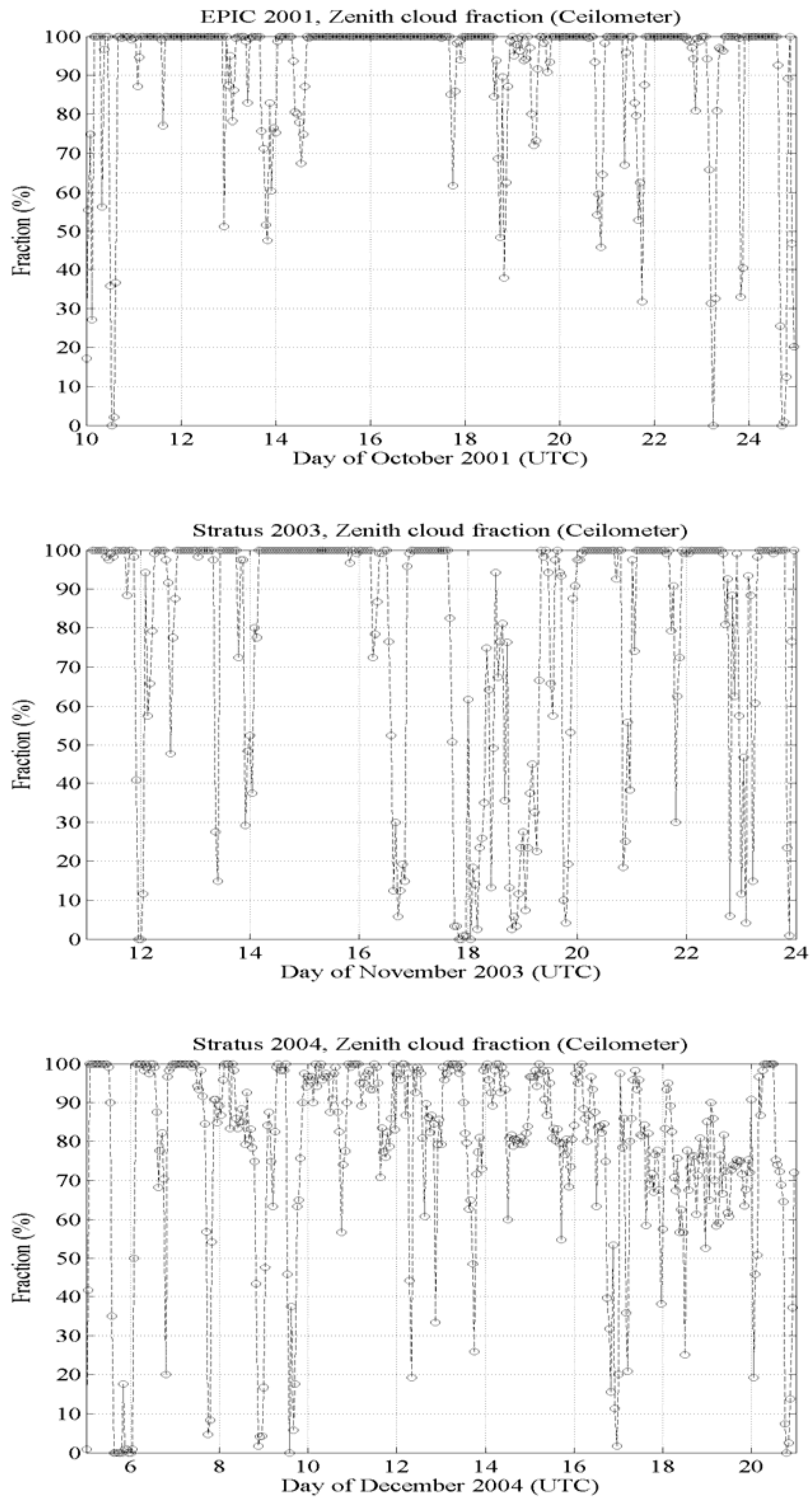

Figure 3. Hourly estimates of zenith-point fractional cloudiness from the ceilometer for EPIC 2001 (top), Stratus 2003 (middle) and Stratus 2004 (bottom). During Stratus 2004, the daytime cloud fraction values were adjusted using the observed downward longwave radiation.

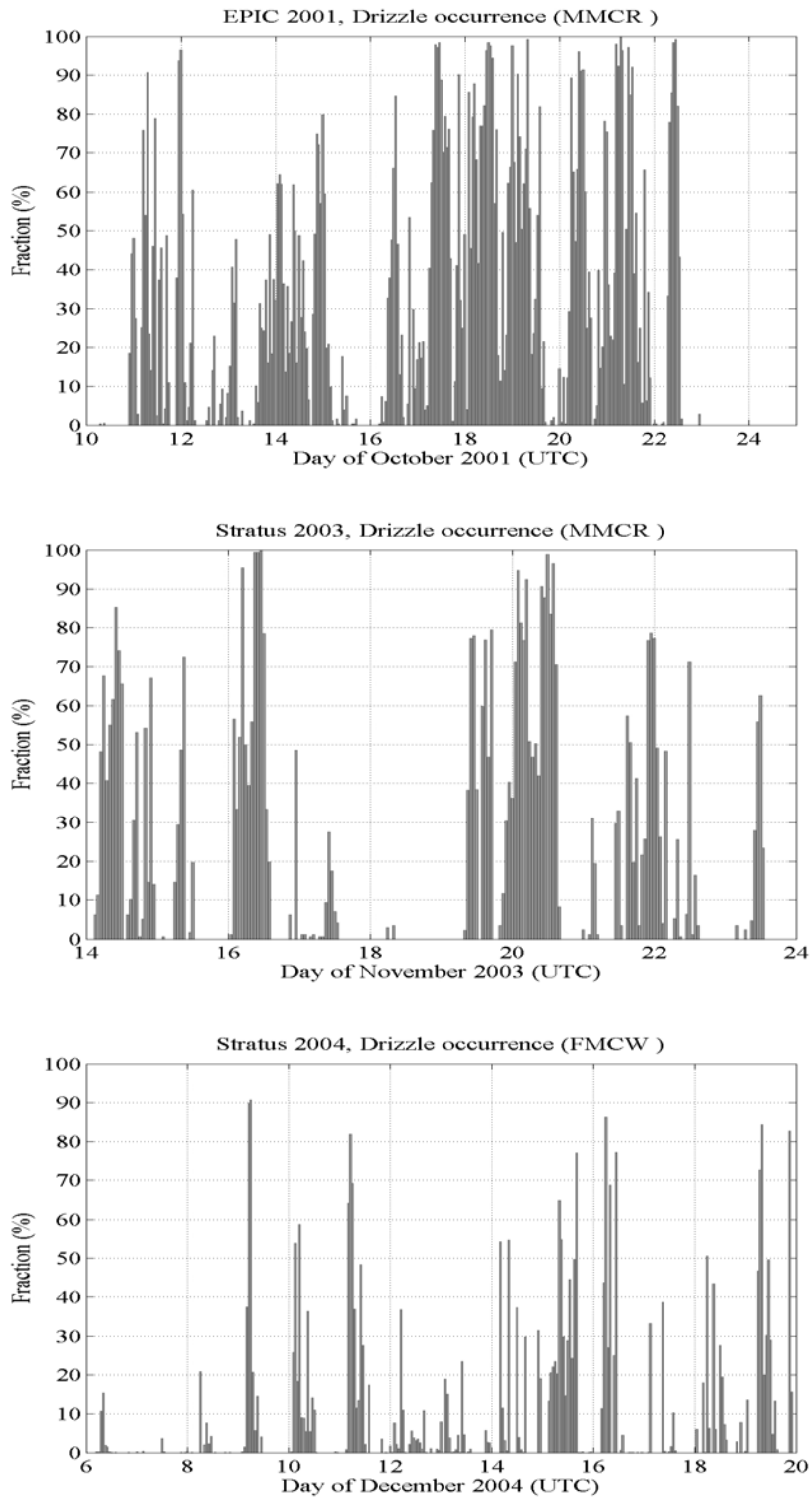

Figure 4. Hourly fractional drizzle occurrence for EPIC 2001 (top), Stratus 2003 (middle) and Stratus 2004 (bottom). Drizzle is defined as MMCR (for EPIC and Stratus 2003) or FMCW (for Stratus 2004) radar profiles having maximum (column-integrated) reflectivity greater than -10 dBZ.

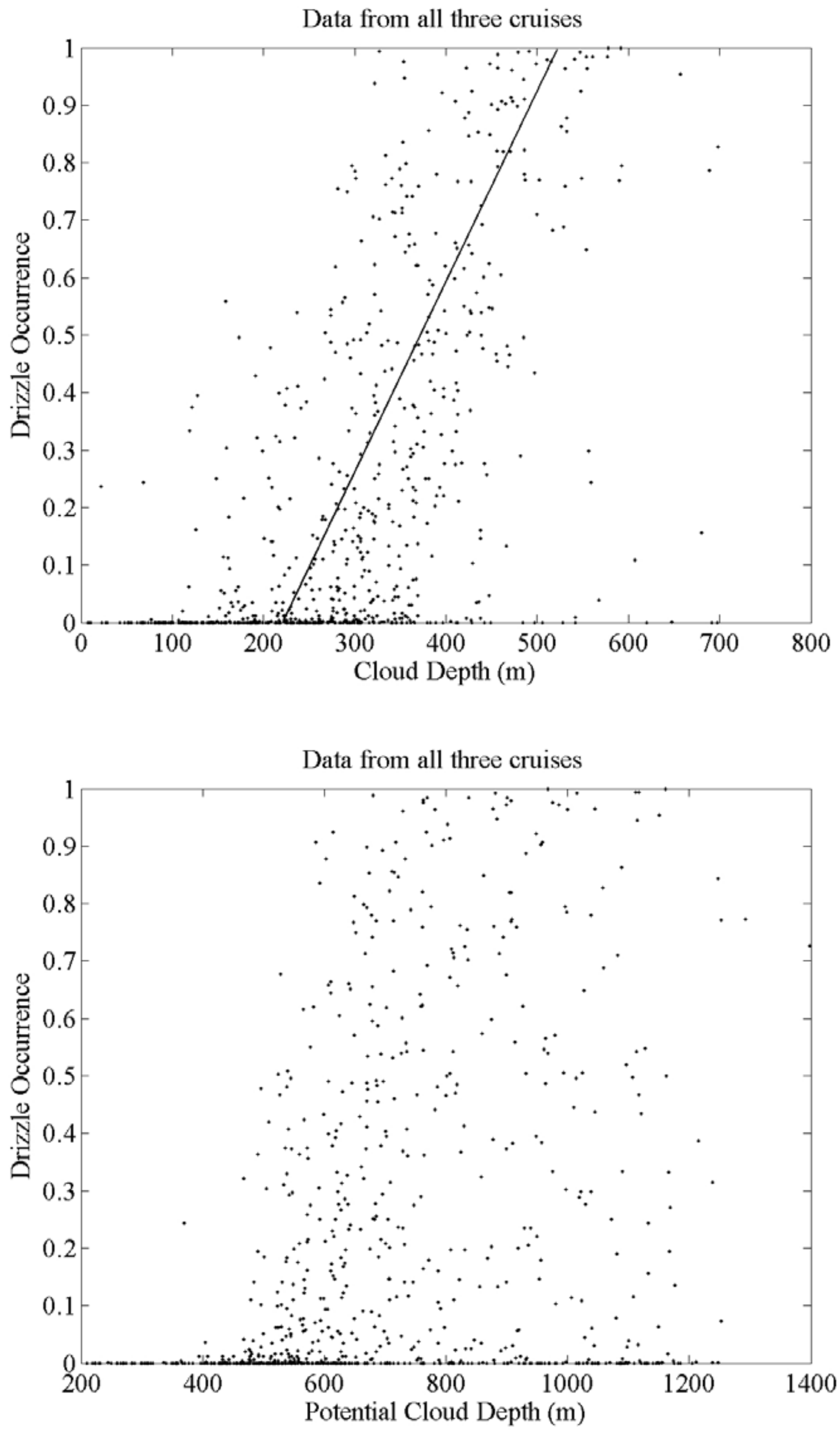

Figure 5. Drizzle Occurrence as a function of cloud depth (upper panel) and potential cloud depth (lower panel). The linear fit in the upper panel is drawn subjectively to avoid the bias on the mathematical calculation imposed by "extreme" domains (e.g. drizzle occurrence equal to zero) as well as the large span of values (the overall correlation coefficient is R=0.61).

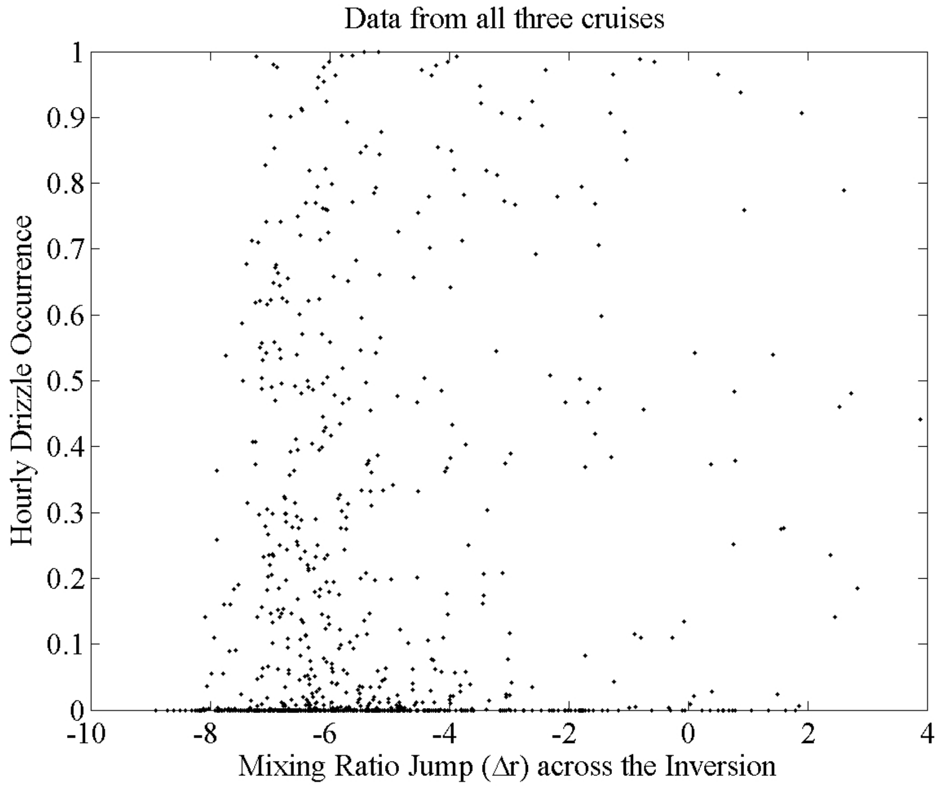

Figure 6. Drizzle occurrence as function of mixing ratio jump across the inversion. The Δr values were initially estimated for each sounding (every 4 or 6 hours, depending on the cruise), then linearly interpolated to the drizzle occurrence hourly estimates.

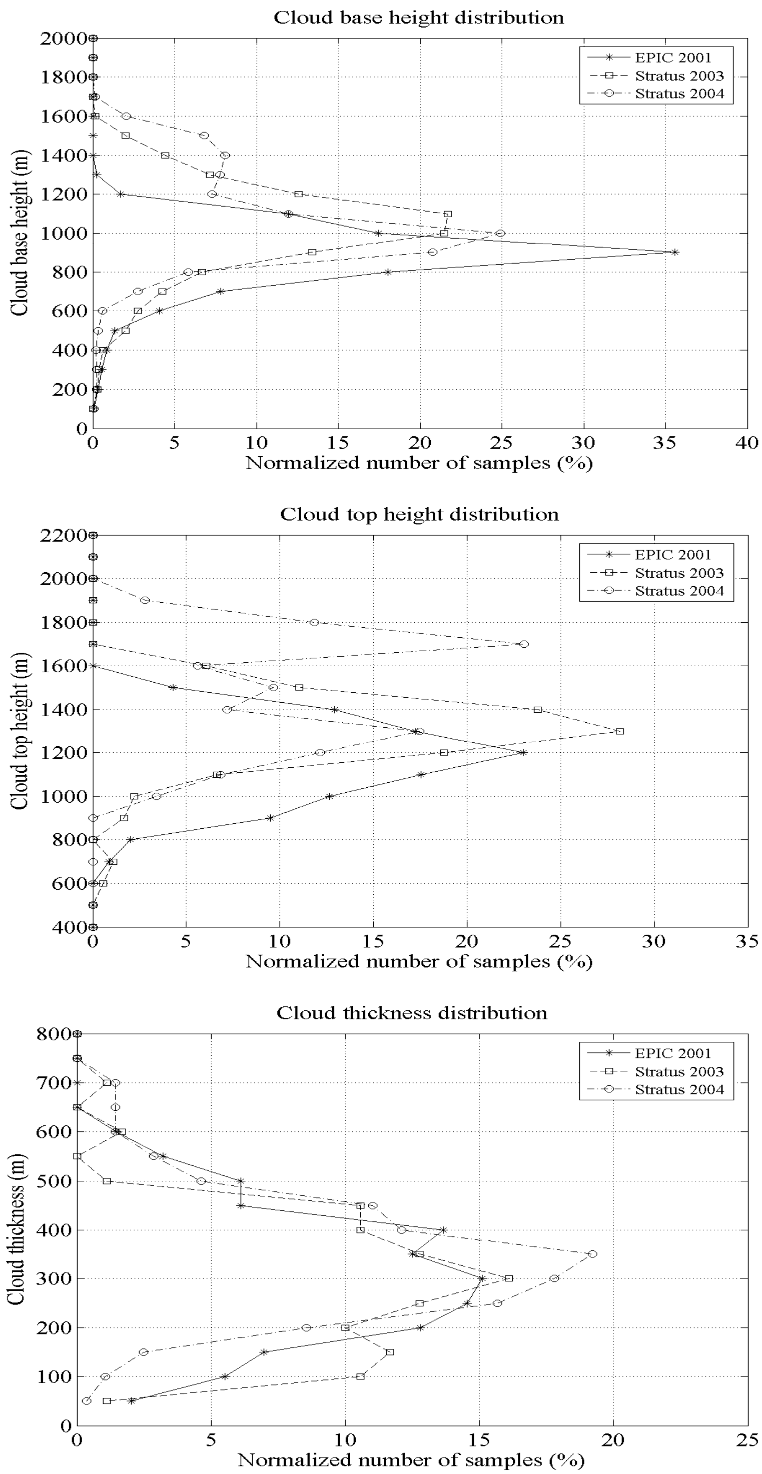

Figure 7. Frequency distributions of cloud properties during EPIC 2001 (stars, solid line), Stratus 2003 (squares, dashed line) and Stratus 2004 (circles, dashed-dotted line). *Upper panel:* Cloud base height distribution in bins of 100m. *Middle panel:* Cloud top height distribution in bins of 100 m. *Lower panel:* Cloud thickness distribution in bins of 50m.

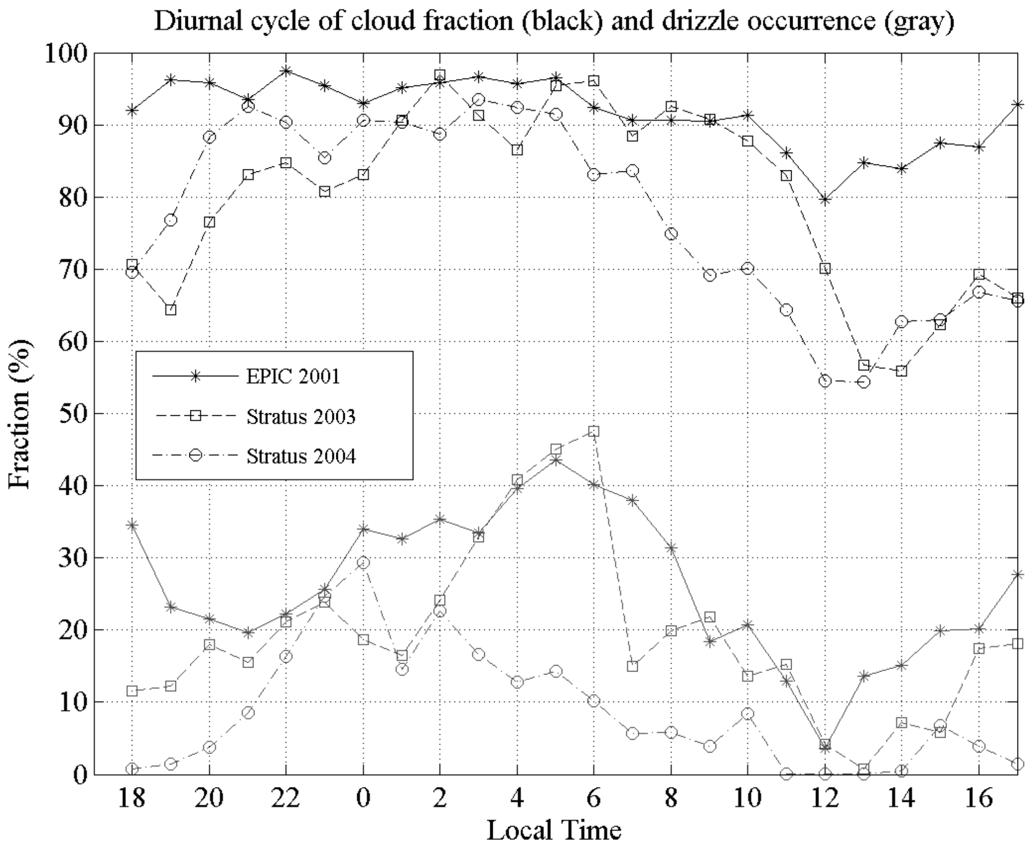

Figure 8. Diurnal cycle of cloud fraction (black-colored lines) and drizzle occurrence (gray-colored lines) during EPIC 2001 (stars, solid line), Stratus 2003 (squares, dashed line) and Stratus 2004 (circles, dashed-dotted line). A -10 dBZ reflectivity threshold is used in the MMCR/FMCW data for the retrieval of the drizzle fraction. The corrected ceilometer data are used for extracting the Stratus 2004 cloud fraction diurnal cycle.

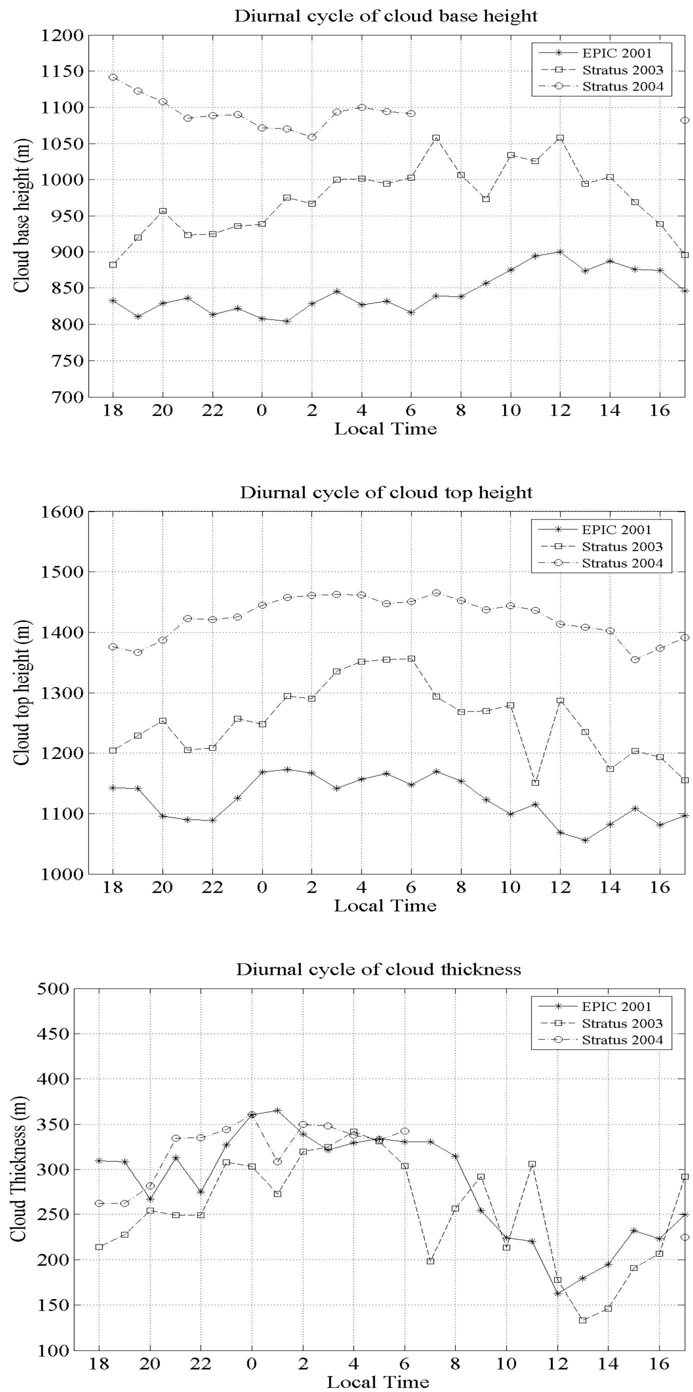

Figure 9. Diurnal cycle of cloud base height (upper panel), cloud top height (middle panel) and cloud thickness (lower panel) during EPIC 2001 (stars, solid line), Stratus 2003 (squares, dashed line) and Stratus 2004 (circles, dashed-dotted line). Cloud thickness is estimated as the difference between the hourly values of cloud top (derived from the MMCR for EPIC 2001 and Stratus 2003, and the wind profiler for Stratus 2004) and cloud base (derived from the ceilometer for all three cruises). Cloud base and cloud thickness estimates for Stratus 2004 daylight hours (0700 to 1600 LT) are not included; cloud base height values are significantly underestimated during these hours due to the respective ceilometer malfunction.

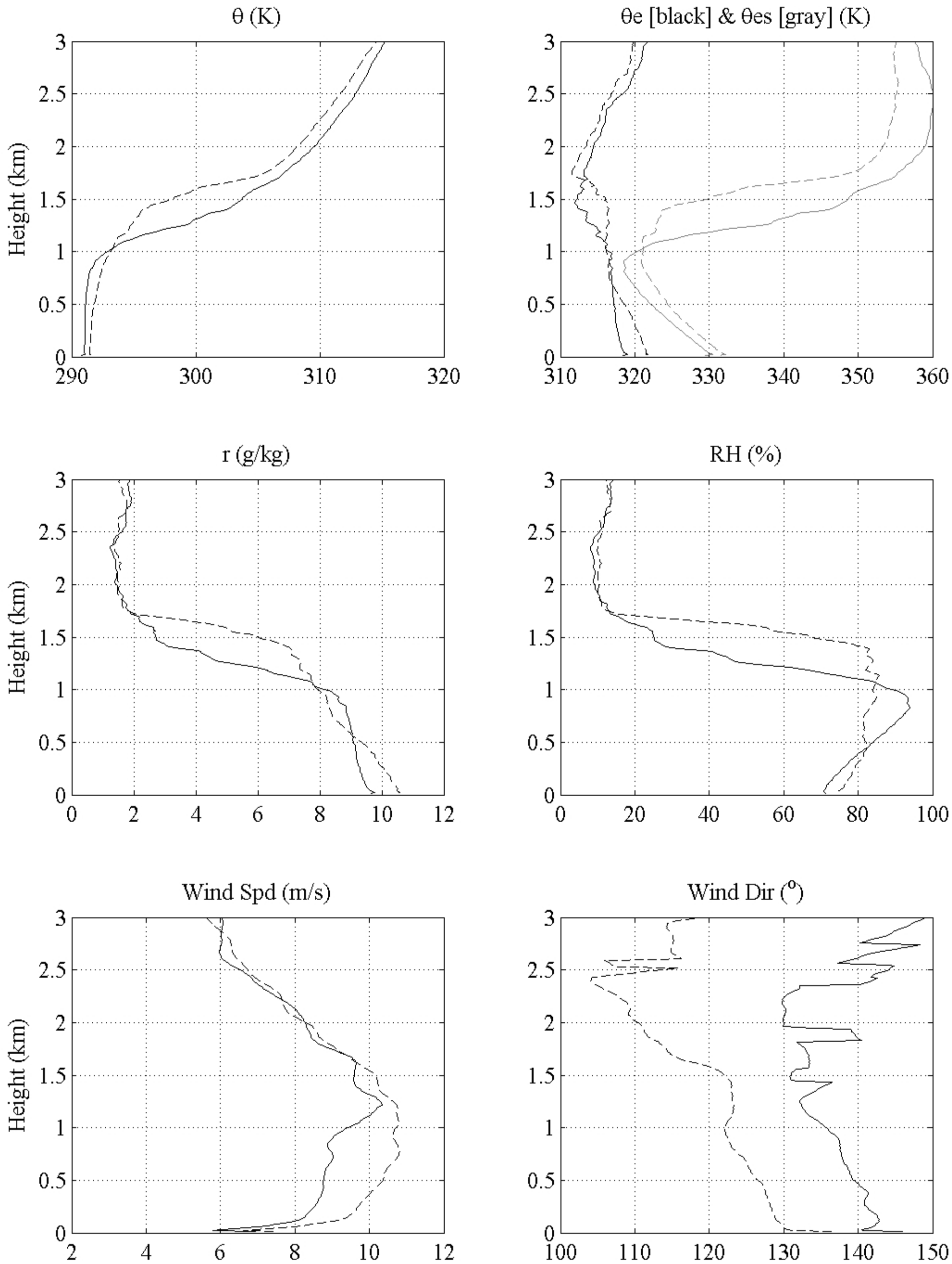

Figure 10. Coupled (solid) vs decoupled (dashed) composite soundings for Stratus 2004. Each variable is noted at the top of each subplot.

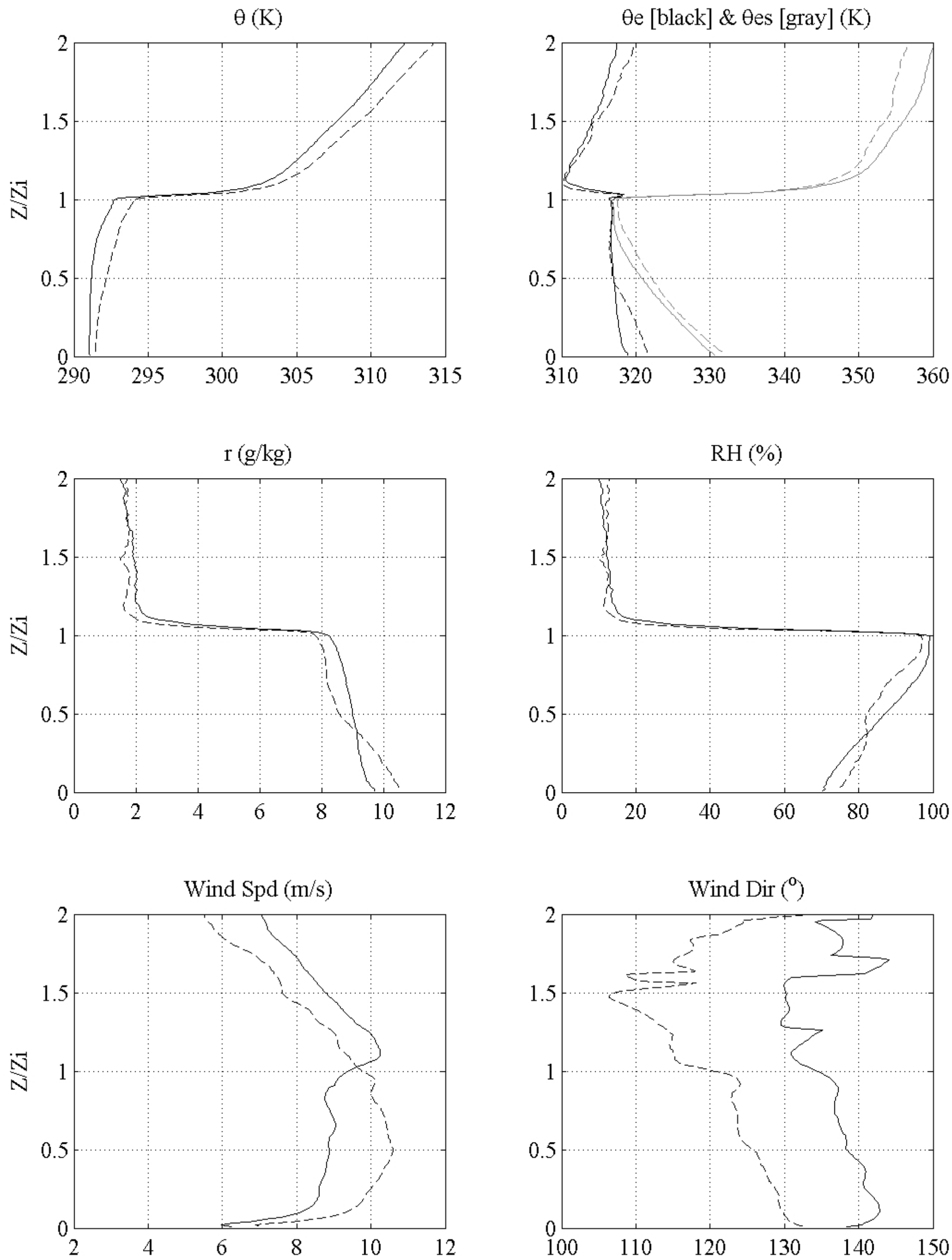

Figure 11. As in Fig. 20, but using height scales normalized by the height of the inversion z_i.

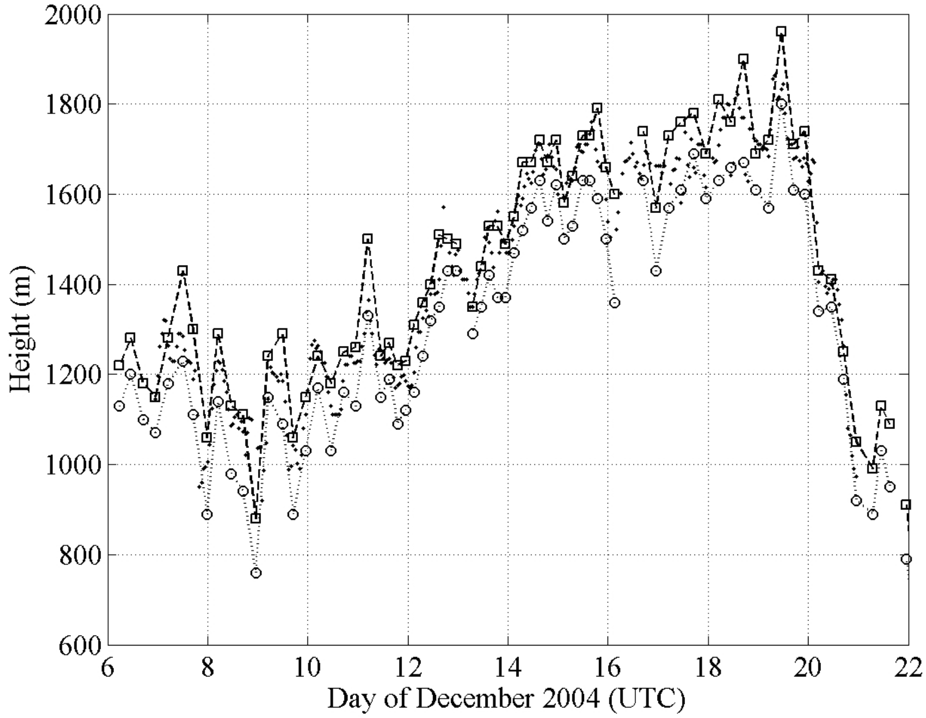

Figure A.1. Comparison of inversion-top (squares – dashed) and inversion-base (circles – dotted) heights from soundings against wind-profiler-derived BL height (dots) for Stratus 2004.

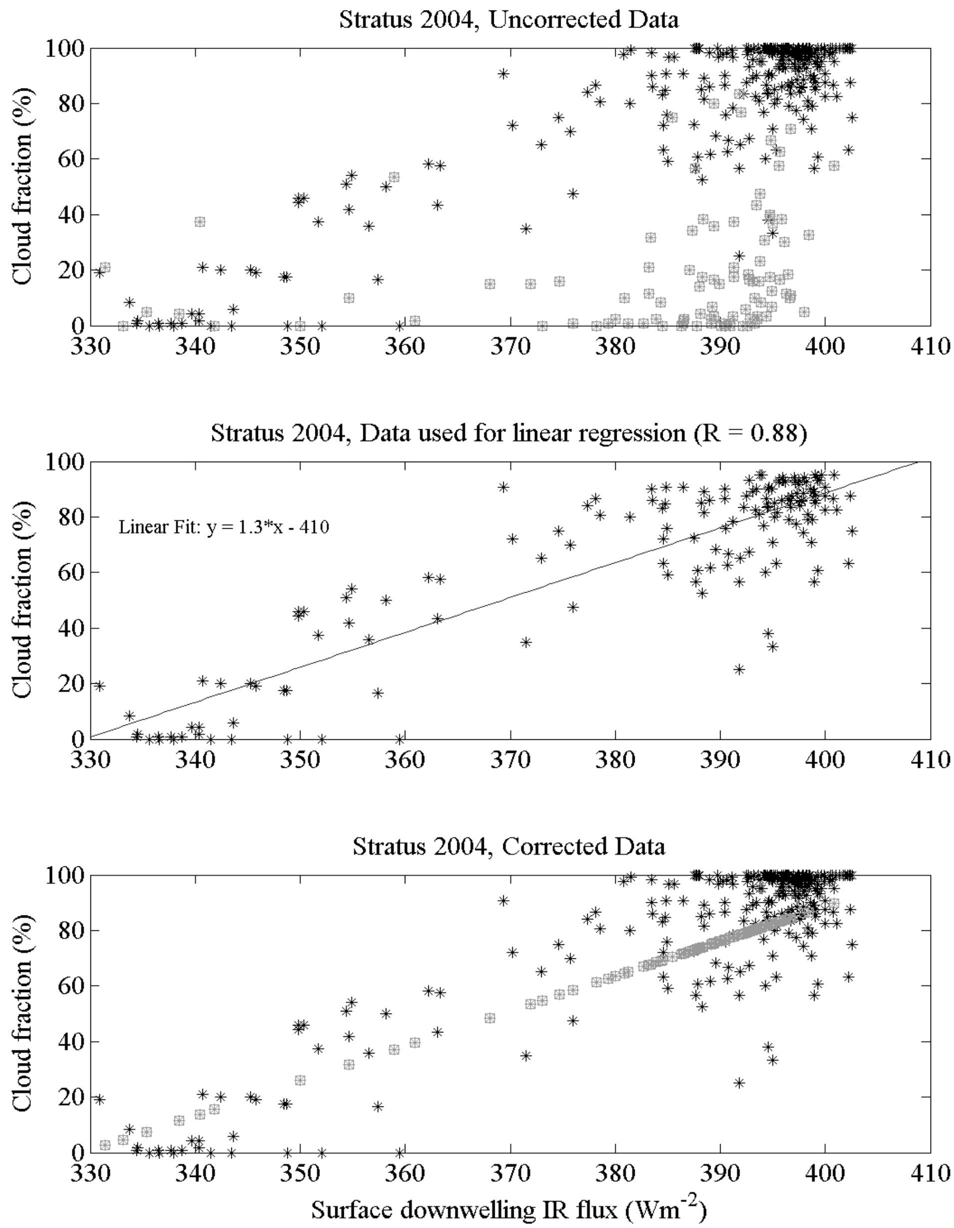

Figure A.2. Analysis procedure followed for extracting accurate cloud-fraction estimates for the time periods affected by the ceilometer malfunction during Stratus 2004. *Upper panel*: The initial (uncorrected) hourly estimates of ceilometer-derived cloud fraction are plotted against the respective hourly-averaged values of incoming longwave radiation (part of the NOAA/ETL air-sea flux system measurements). Data points corresponding to intervals affected by ceilometer malfunction are marked with gray squares. *Middle panel*: Same as before, but only including "problem-free" data points with cloud fraction values less than 95%. The linear least-squares fit is plotted with a straight line, and the respective equation and correlation coefficient are also displayed. *Lower panel*: The linear fit is used to estimate the cloud fraction value for the affected data points, identified before (marked with gray squares).

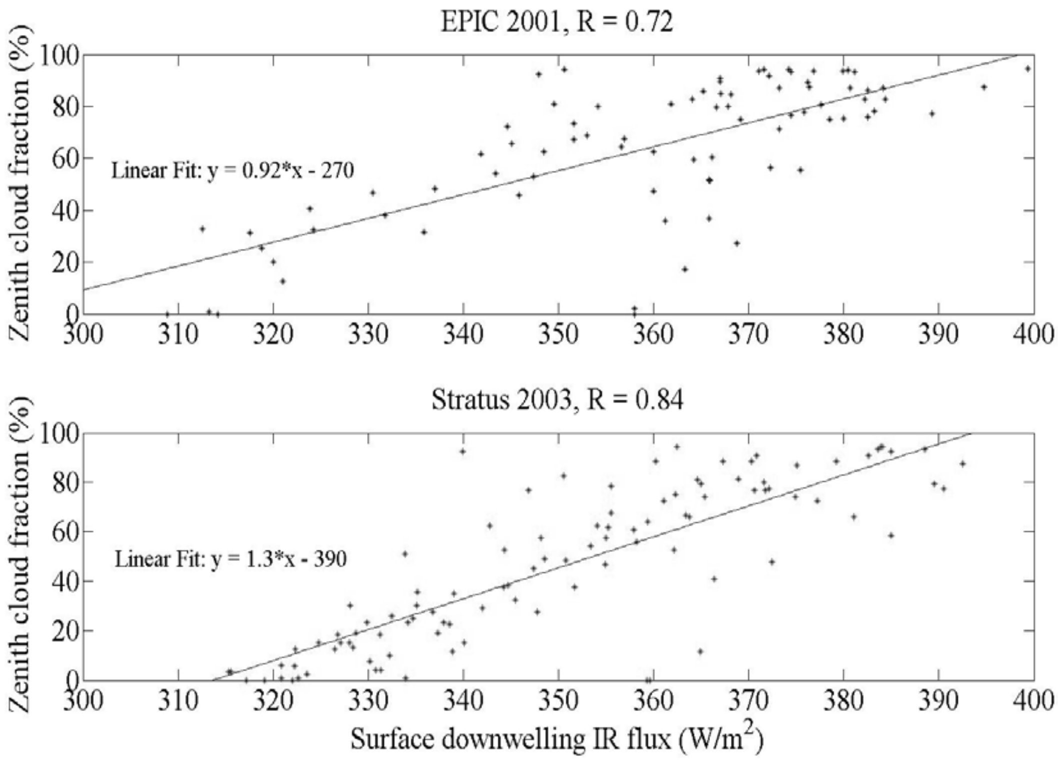

Figure A.3. Surface longwave radiative flux as a surrogate of zenith cloud fraction for EPIC (upper panel) and Stratus 2003 (lower panel). The linear fits are plotted with straight lines, and the respective equations and correlation coefficients are also displayed. Values of cloud fraction greater than 95% have been excluded to improve the linear fits.

Table 1. Time schedule for the 3 stratus cruises.

	EPIC 2001	Stratus 2003	Stratus 2004
Cruise period (dates)	Oct. 9-25	Nov. 11-24	Dec. 5-23
Buoy period (dates)	Oct. 16-22	Nov. 15-21	Dec. 11-16
Exact time of arrival (at the buoy)	(Oct.) 15.955	(Nov.) 15.781	(Dec.) 11.181
Exact time of departure (from the buoy)	(Oct.) 22.330	(Nov.) 21.375	(Dec.) 16.250

Table 2 A list of the remote sensing instruments onboard the *Brown* and the *Revelle* and the respective products.

Sensor	Research cruise	Technical specifications	Direct products	Derived quantities
FMCW* radar	Stratus 2004	94-GHz (3.2 mm) – Vertically pointing	Reflectivity, Doppler Velocity, Doppler Spectrum Width	Drizzle occurrence (Stratus 2004)
MMCR** pulse radar	All three	35-GHz (8.6 mm) – vertically pointing	Reflectivity, Doppler velocity, Doppler spectrum width	Cloud-top height, Drizzle occurrence (EPIC – Stratus 2003)
Brown C-Band radar	EPIC 2001, Stratus 2004	5.6-GHz (5.4 cm) – Scanning	Reflectivity and radial velocity	N/A
Wind Profiler	EPIC 2001, Stratus 2004	915-MHz (32.8 cm)	Reflectivity, wind speed and direction	Cloud top height (Stratus 2004)
Ceilometer	All three	Lidar (Vaisala CT-25K)	Backscatter, cloud base height	Cloud Fraction
Microwave Radiometer	All three	3-channels: 20.6, 31.6, 90 GHz	Column integrated liquid and vapor	N/A

* Frequency Modulated Continuous Wave

** Millimeter Cloud Radar

Table B. 1. Composite soundings used in this study at intervals of 0.1 z/z_i

	EPIC Composite			Stratus 2003 Composite			Stratus 2004 Composite		
z/z_i	P(mbar)	θ(K)	r(g kg^{-1})	P(mbar)	θ(K)	r(g kg^{-1})	P(mbar)	θ(K)	r(g kg^{-1})
0.1	1004.6	289.03	8.51	998.6	290.44	9.51	1000.6	291.57	10.19
0.2	990.3	289.13	8.40	984.5	290.55	9.31	984.3	291.65	9.85
0.3	976.2	289.17	8.29	970.5	290.66	9.10	968.3	291.71	9.61
0.4	962.2	289.23	8.21	956.7	290.90	8.82	952.4	291.87	9.20
0.5	948.3	289.30	8.15	943.0	291.09	8.60	936.7	292.08	8.80
0.6	934.6	289.42	8.05	929.6	291.33	8.45	921.3	292.26	8.66
0.7	921.1	289.63	7.98	916.2	291.66	8.24	906.0	292.53	8.48
0.8	907.7	290.04	7.82	903,0	291.97	8.11	890.9	292.82	8.38
0.9	894.5	290.62	7.61	890.0	292.49	7.94	876.0	293.36	8.28
1.0	881.4	291.28	7.27	877.1	293.37	7.50	861.4	293.88	8.02
1.1	868.7	298.94	1.69	864.6	300.69	2.85	847.1	303.71	2.33
1.2	856.3	302.93	1.20	852.3	302.71	2.04	833.3	305.55	1.72
1.3	844.1	304.48	1.14	840.3	303.90	2.44	819.7	306.86	1.76
1.4	832.1	305.73	0.99	828.4	305.02	2.51	806.3	308.08	1.66
1.5	820.2	306.84	1.01	816.7	305.94	2.38	793.1	309.23	1.73
1.6	808.6	307.81	1.07	805.2	306.77	2.27	780.1	310.36	1.81
1.7	797.1	308.62	1.15	793.8	307.67	1.87	767.3	311.33	1.63
1.8	785.7	309.24	1.21	782.5	308.33	1.60	754.7	312.36	1.67
1.9	774.5	309.78	1.38	771.4	308.98	1.58	742.3	313.25	1.81
2.0	763.4	310.29	1.49	760.4	309.82	1.30	730.1	314.24	1.90

Table B. 2. Buoy period statistics.

			EPIC		Stratus 2003		Stratus 2004	
			Mean	*Std*	*Mean*	*Std*	*Mean*	*Std*
Soundings	Surface 1000 mb	Temperature T (K)	289.1	0.6	290.4	0.6	291.6	0.3
		Pot. Temp. θ (K)	289.1	0.6	290.4	0.6	291.6	0.3
		Vir. Pot. Temp. θ_v (K)	290.6	0.6	292.1	0.6	293.4	0.3
		Eq. Pot. Temp. θ_e (K)	313.3	1.6	317.7	2.7	320.8	2
		Sat. Eq. Pot. Temp. θ_{es} (K)	321.5	1.8	325.9	2	329.9	1.1

		Mix. Ratio *r* (g kg^{-1})	8.5	0.6	9.6	1	10.2	0.8
		Rel. Humidity (%)	74.4	6.5	76.9	8	76.1	6
		Wind Speed (m s^{-1})	7.7	2.2	6.8	1.7	9.7	1.3
		Wind Direction (°)	119	14	121	17	129	9
	700 mb	Temperature *T* (K)	283.7	0.6	283.1	1.1	285.2	1.2
		Pot. Temp. θ (K)	314.1	0.6	313.4	1.2	315.7	1.3
		Vir. Pot. Temp. θ_v (K)	314.3	0.7	313.6	1.1	316.1	1.3
		Eq. Pot.	317.	2.	316.	1.8	322.	4.2

	Temp. θ_e (K)	9	8	2		5	
	Sat. Eq. Pot. Temp. θ_{es} (K)	350.1	2	348.1	3.9	355.9	4.7
	Mix. Ratio r (g kg^{-1})	1.1	0.8	0.8	0.6	2	1.3
	Rel. Humidity (%)	9.6	6.5	7.4	6.3	15.9	10.2
	Wind Speed (m s^{-1})	4.5	2	4.8	2.2	6.4	2.5
	Wind Direction (°)	140	60	155	85	120	16
Inversion	Inversion Base Height	1218	105	1208	152	1403	163

		(m)						
		Inversion Top Height (m)	1403	123	1311	166	1521	168
		Inversion $\Delta\theta$ (K)	10.5	2.5	7.1	2.4	9.6	1.1
		Inversion Δr (g kg^{-1})	-5.9	1.2	-4.5	1.9	-5.2	2.3
		Inversion shear (m s^{-1})	-0.78	1	-0.5	1.3	0	1.5
Ceilometer		Cloud Base Height (m)	922	88	953	230	1104	185
		Zenith Cloud Fraction (%)	94.1	-	66.1	-	86.5	14.9

Radar	Cloud top Height (m)	1255	113	1233	184	1474	170
	Drizzle Occurrence	42.9	34	22.3	33.2	10.6	18.2
Radar-Ceilometer	Cloud Thickness (m)	341	118	276	142	323	134
Air-Sea Flux System	*SST* (°C)	18.6	0.1	19.3	0.2	19.5	0.1
	SST-T_{air} (°C)	1.6	0.6	0.6	0.5	0.1	0.3
	Surf. Sea Spec. Hum. q_{sea} (g kg^{-1})	13.1	0.1	13.6	0.2	13.9	0.1
	q_{sea}-q_{air} (g kg^{-1})	4.1	0.6	3.3	0.9	3.5	0.6
	Surf. Inc. Solar flux	223	32	288	37	202	28

	(W m^{-2})		3		7		1
	Surf. Inc. IR flux (W m^{-2})	383	17	364	30	393	10
	Sensible Heat Flux (W m^{-2})	14	7	2	5	-2	3
	Latent Heat Flux (W m^{-2})	99	19	68	27	83	19
	Virtual Heat Flux (W m^{-2})	21	7	7	5	4	3